

Supporting Information

Development of *N*-(Functionalized Benzoyl)-homocycloleucyl-glycinonitriles as Potent Cathepsin K Inhibitors

Jure Borišek,[†] Matej Vizovišek,[‡] Piotr Sosnowski,[‡] Boris Turk,^{‡,||,§} Dušan Turk,^{*,‡,§} Barbara Mohar,[†] and Marjana Novič^{*,†}

[†]National Institute of Chemistry, Hajdrihova 19, SI-1001 Ljubljana, Slovenia

[‡]Department of Biochemistry, Molecular and Structural Biology, Jozef Stefan Institute, Jamova cesta 39, SI-1000 Ljubljana, Slovenia

[§]Centre of Excellence for Integrated Approaches in Chemistry and Biology of Proteins, Jamova cesta 39, SI-1000 Ljubljana, Slovenia

^{*}Faculty of Chemistry and Chemical Technology, University of Ljubljana, Slovenia

Table of Contents

Table S1	S2
Table S2	S2
Table S3	S3
Table S4	S4
Scheme S1	S5
Figure S1	S6
Figure S2	S7
Figure S3	S8
Figure S4	S9
NMR spectra	S10

Table S1. Distribution of the various *N*-(functionalized benzoyl)-homocycloleucyl-glycinonitriles in the virtual combinatorial library.

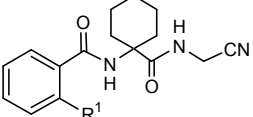
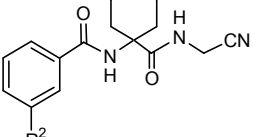
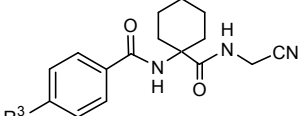
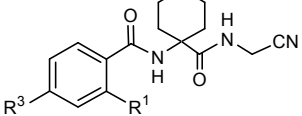
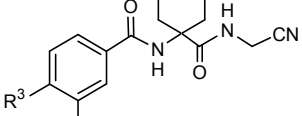
Virtual compound structure	Number of virtual compounds
	39
	46
	94
	18
	57
Total: 254	

Table S2. The post-docking analysis of the experimental and combinatorial datasets using the 4DMX binding site and the consensus results (merged post-docking and QSAR evaluation of the combinatorial dataset).

For this, see the appended Excel file.

Table S3. Molecular docking-calculated H-bond lengths (\AA) between Cat K and compound **5**, **6**, or **9**.

Cat K amino acid residue	Compound atom	H-bond length with compound 5	H-bond length with compound 6	H-bond length with compound 9
Cys25	C1	1.66	n.i.	1.77
Gln19	N1	3.02	n.i.	3.01
Asn161	N3	3.01	3.21	3.06
Gly66	O5	3.11	2.91	3.16
Gly66	N12	2.73	3.18	3.01
Gly64	N21	2.90	2.87	n.i.
Asn117 ^(b)	N21 ^(a)	2.53	3.20	n.i.
Asp61 ^(b)	F22 ^(a)	n.i.	n.i.	3.05
Glu118 ^(b)	F22 ^(a)	n.i.	n.i.	3.06

^a First asymmetric unit of cathepsin K crystal structure.

^b Second asymmetric unit of cathepsin K crystal structure.

n.i.: no interaction.

Table S4. Data and refinement statistics extracted by Phenix software.¹

Cat K -"Ligand" complex	Compound 5	Compound 6	Compound 9
Wavelength (Å)	1.584	1.584	1.0
Resolution range (Å)	45.99 - 1.59 (1.642 - 1.585)	46.28-1.87 (1.937-1.87)	46.37 - 1.0 (1.036 - 1.0)
Space group	P 1 21 1	P 21 21 21	P 21 21 21
Unit cell	47.22 90.00	44.40 90.00	51.35 90.00
Total reflections	49603 (4338)	141950 (10892)	540950 (25908)
Unique reflections	25360 (2388)	14804 (1469)	92375 (6766)
Multiplicity	1.9 (1.8)	9.5 (7.4)	5.9 (3.8)
Completeness (%)	97.53 (90.01)	98.31 (916)	96.78 (71.72)
Mean I/sigma(I)	9.12 (1.17)	9.96 (3.78)	15.89 (1.79)
Wilson B-factor	13.81	8.42	8.34
R-merge	0.08534 (1.124)	0.2593 (0.9815)	0.05199 (0.5977)
R-work	0.1896 (0.3436)	0.1810 (0.2420)	0.1115 (0.2151)
R-free	0.2414 (0.3366)	0.2371 (0.3690)	0.1351 (0.2057)
Number of non-hydrogen atoms	2004	1909	2118
Protein residues	215	215	215
RMS (bonds)	0.019	0.019	0.022
RMS (angles)	1.91	1.76	2.10
Ramachandran favoured (%)	97	97	97
Ramachandran outliers (%)	0	0	0
Clashscore	3.12	3.31	3.01
Average B-factor	19	9	13.4
macromolecules	17.3	7.9	10.3
ligands	25.6	15.20	14.7
solvent	30.6	16.40	33.5

Statistics for the highest-resolution shell are shown in parentheses.

(1) (a) Afonine, P.V.; Grosse-Kunstleve, R.W.; Echols, N.; Headd, J.J.; Moriarty, N.W.; Mustyakimov, M.; Terwilliger, T.C.; Urzhumtsev, A.; Zwart, P.H.; Adams, P.D. Towards automated crystallographic structure refinement with phenix.refine. *Acta Crystallogr. D* **2010**, *68*, 352–367.

(b) Adams, P.D.; Afonine, P.V.; Bunkoczi, G.; Chen, V.B.; Davis, I.W.; Echols, N.; Headd, J.J.; Hung, L.W.; Kapral, G.J.; Grosse-Kunstleve, R.W.; McCoy, A.J.; Moriarty, N.W.; Oeffner, R.; Read, R.J.; Richardson, D.C.; Richardson, J.S.; Terwilliger, T.C.; Zwart, P.H. PHENIX: a comprehensive Python-based system for macromolecular structure solution. *Acta Crystallogr. D* **2010**, *66*, 213–221.

Scheme S1. General synthetic pathway for the virtual combinatorial library of the *N*-(functionalized benzoyl)-homocycloleucyl-glycinonitriles.

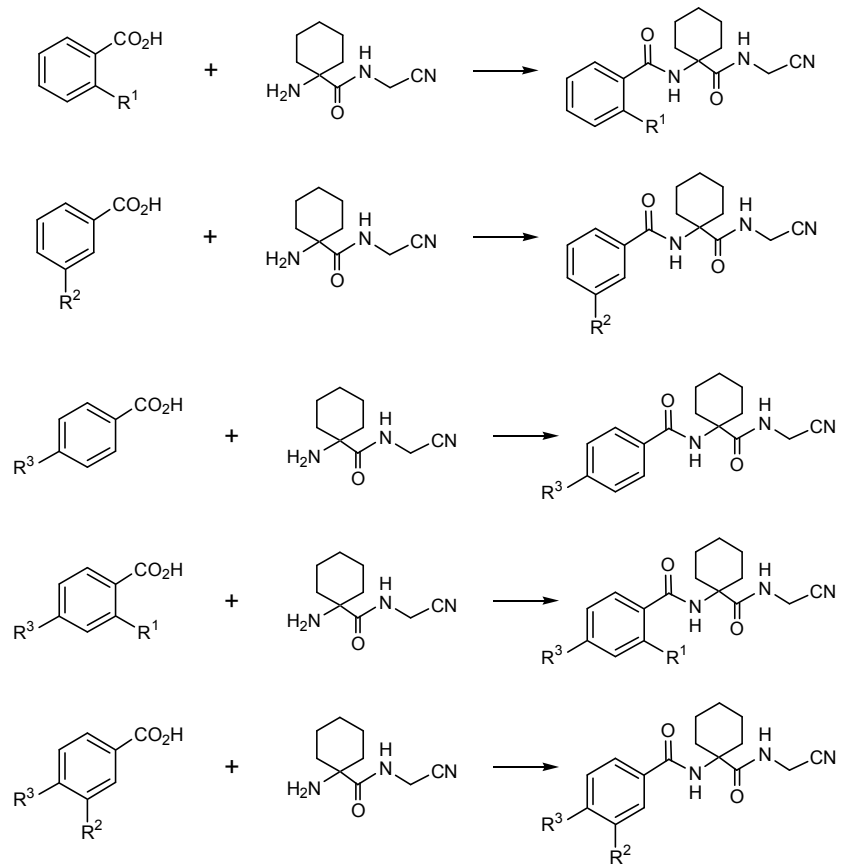


Figure S1. 0LB ligand.

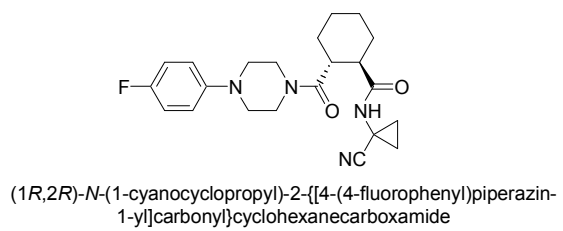


Figure S2. Reversibility of cathepsin K inhibition by compounds **5**, **6** and **9**. After 30 minutes of incubation of 1 μ M cathepsin K with 5 μ M compounds **5**, **6** or **9** (final concentration), the complex was rapidly diluted 100-fold in the reaction medium containing 50 μ M Z-Gly-Pro-Arg-AMC, followed by monitoring substrate hydrolysis. E-64 was included as a control for irreversible inhibition. Substrate hydrolysis is plotted as relative fluorescence units (RFU) versus time. The solid curves represent the best fit to the equation $[P] = v_{st} + (v_o - v_s)(1 - e^{-kt})/k$. All other experimental conditions were as described under Experimental section.

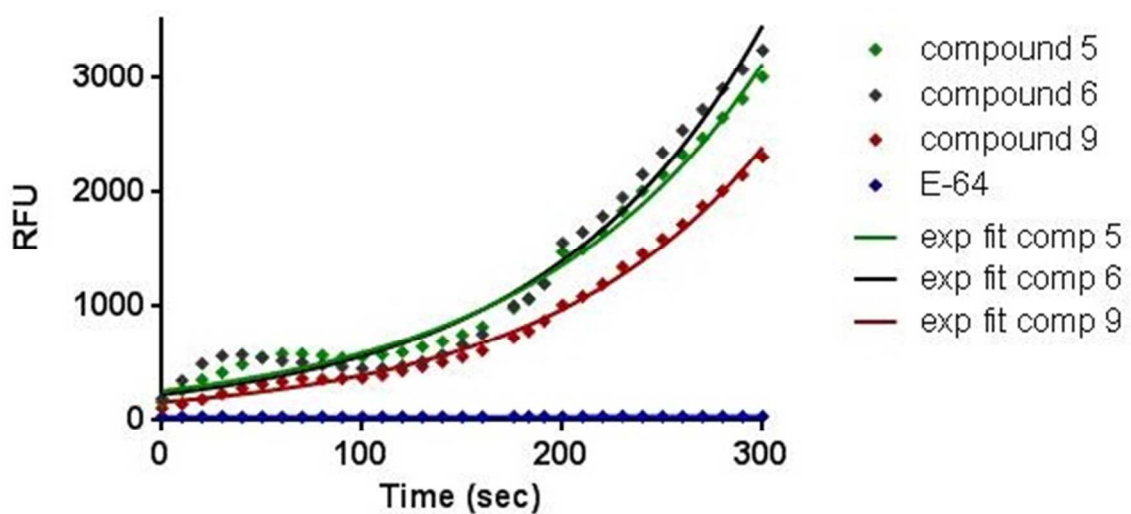
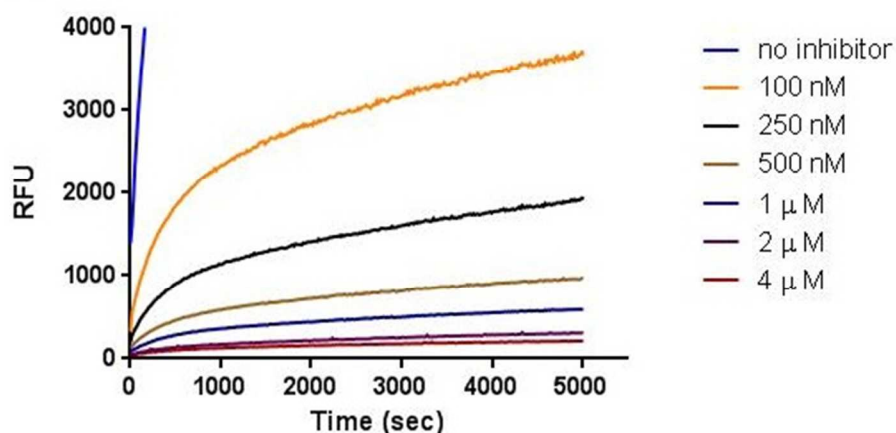
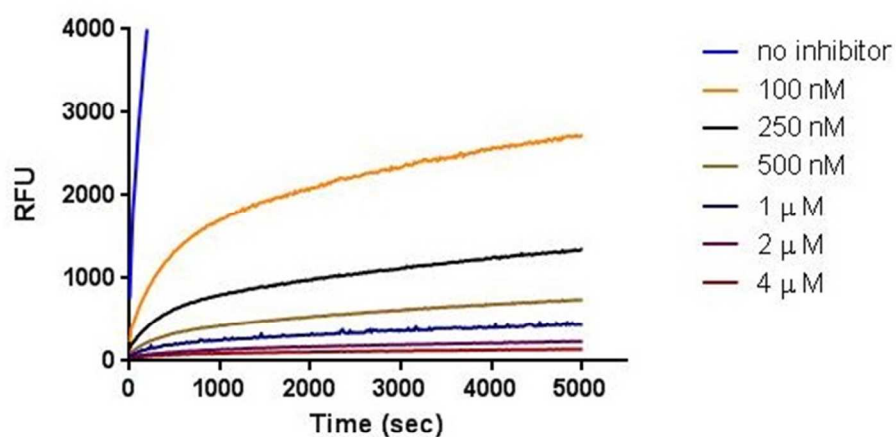


Figure S3. Progress curves for inhibition of cathepsin K by compounds **5**, **6** and **9**:
 (a) compound **5**; (b) compound **6**; (c) compound **9**. All experimental details are given in the Experimental Section (In vitro inhibition assay; Kinetics of Cat K inhibition by compounds **5**, **6** and **9**).

a.



b.



c.

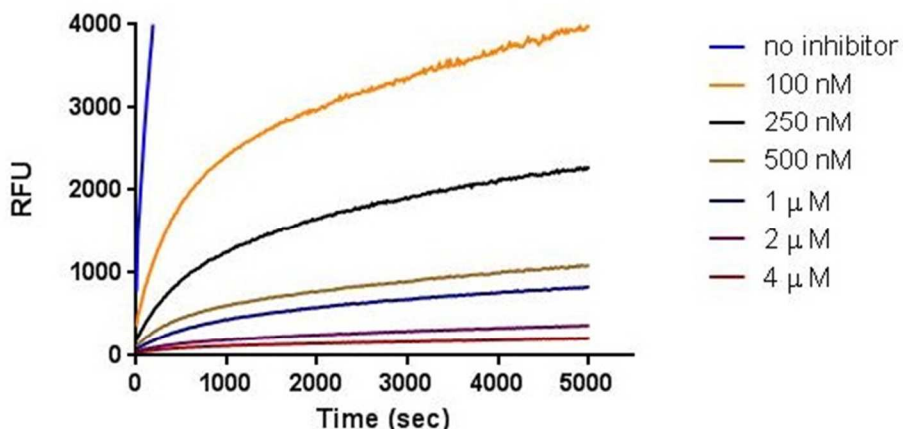
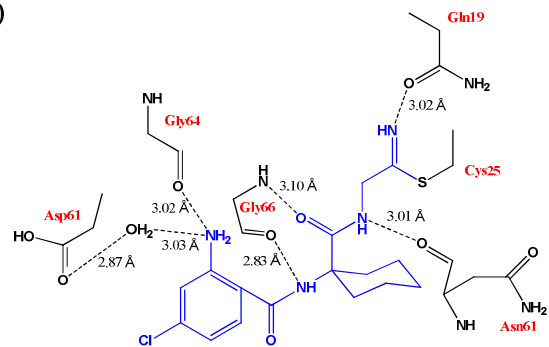


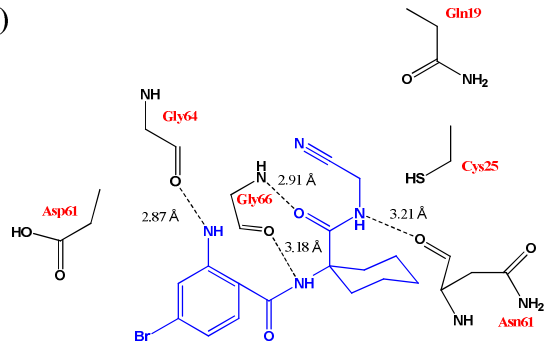
Figure S4. 2D representation of the key interactions (H-bonds) and distances in the crystal structures of cathepsin K: (a) for compound **5**, (b) for compound **6**, and (c) for compound **9**. Alternate conformation (noncovalent binding mode) of compound **9** and its interactions are colored in magenta.

a)



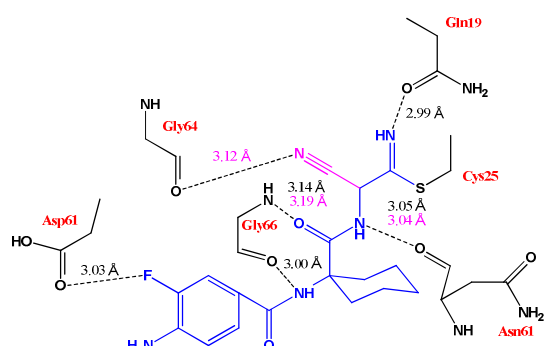
compound **5**

b)



compound **6**

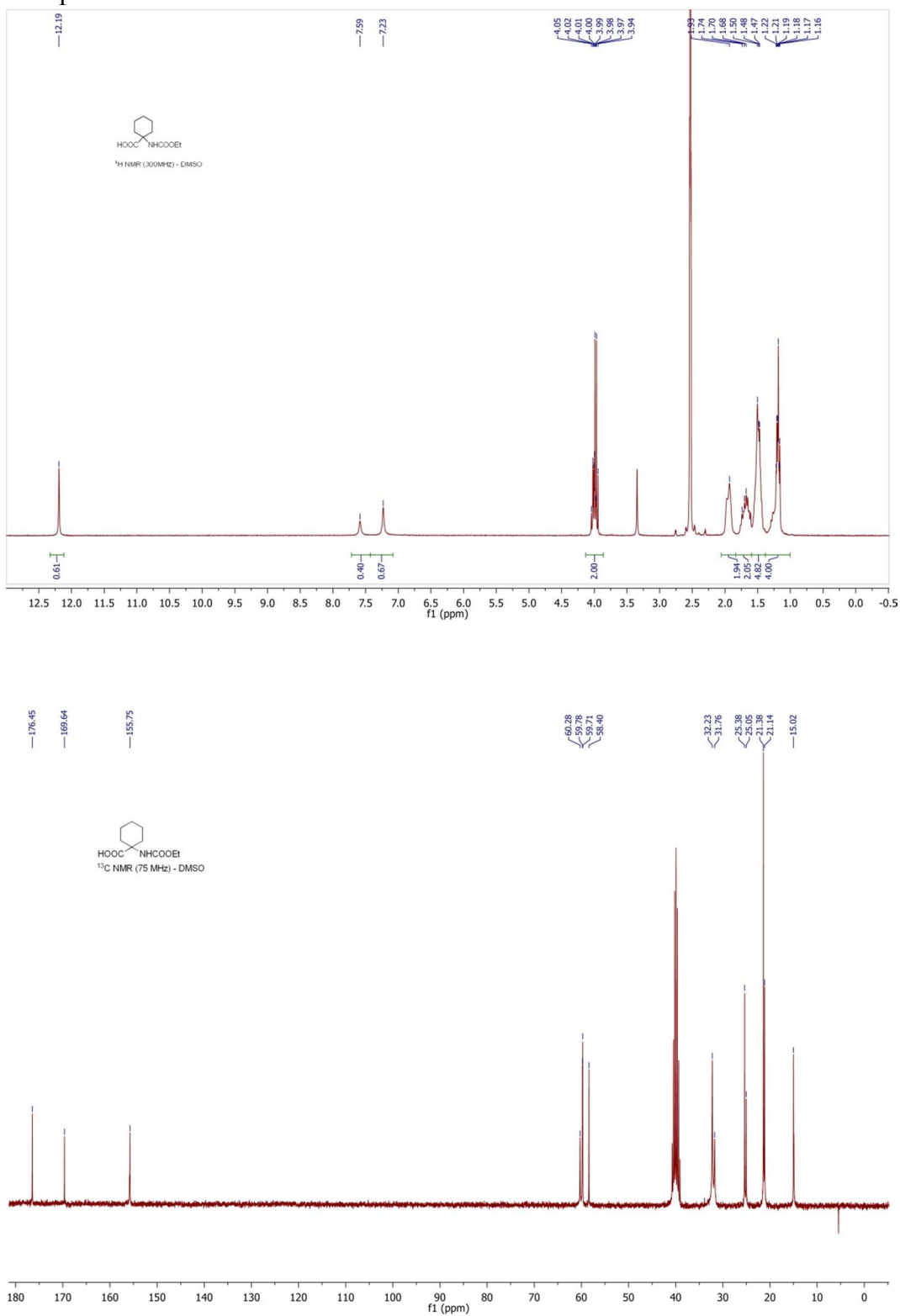
c)



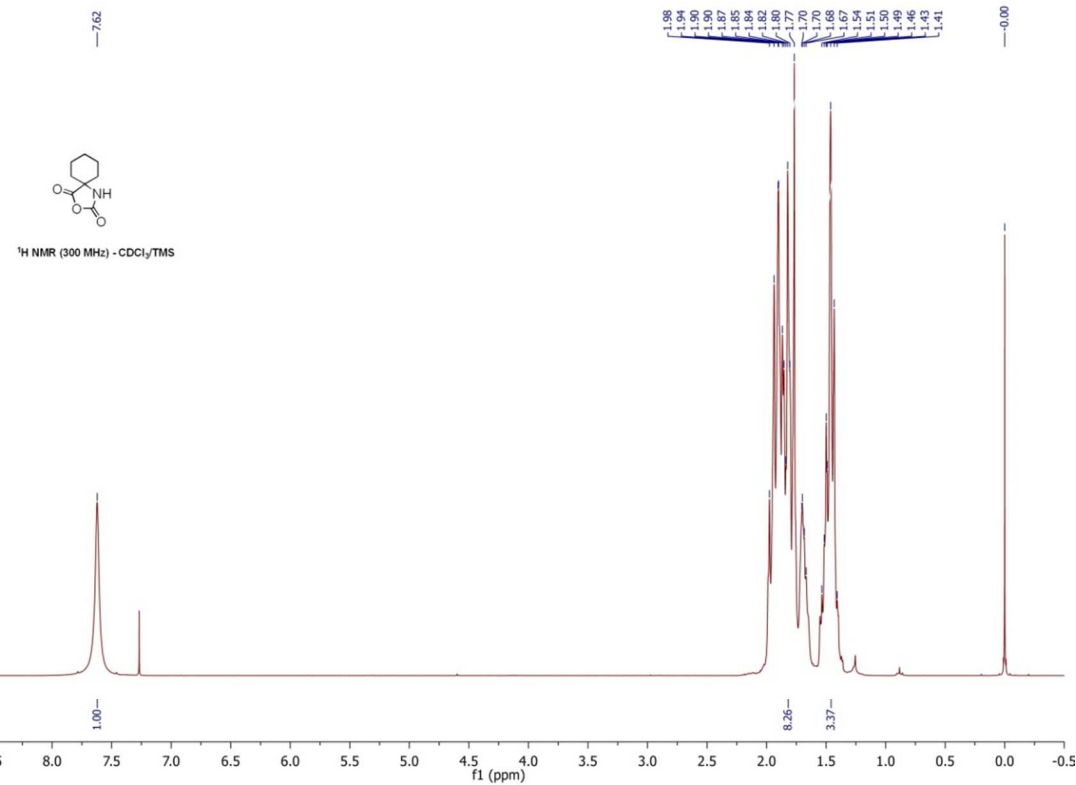
compound **9**

NMR spectra

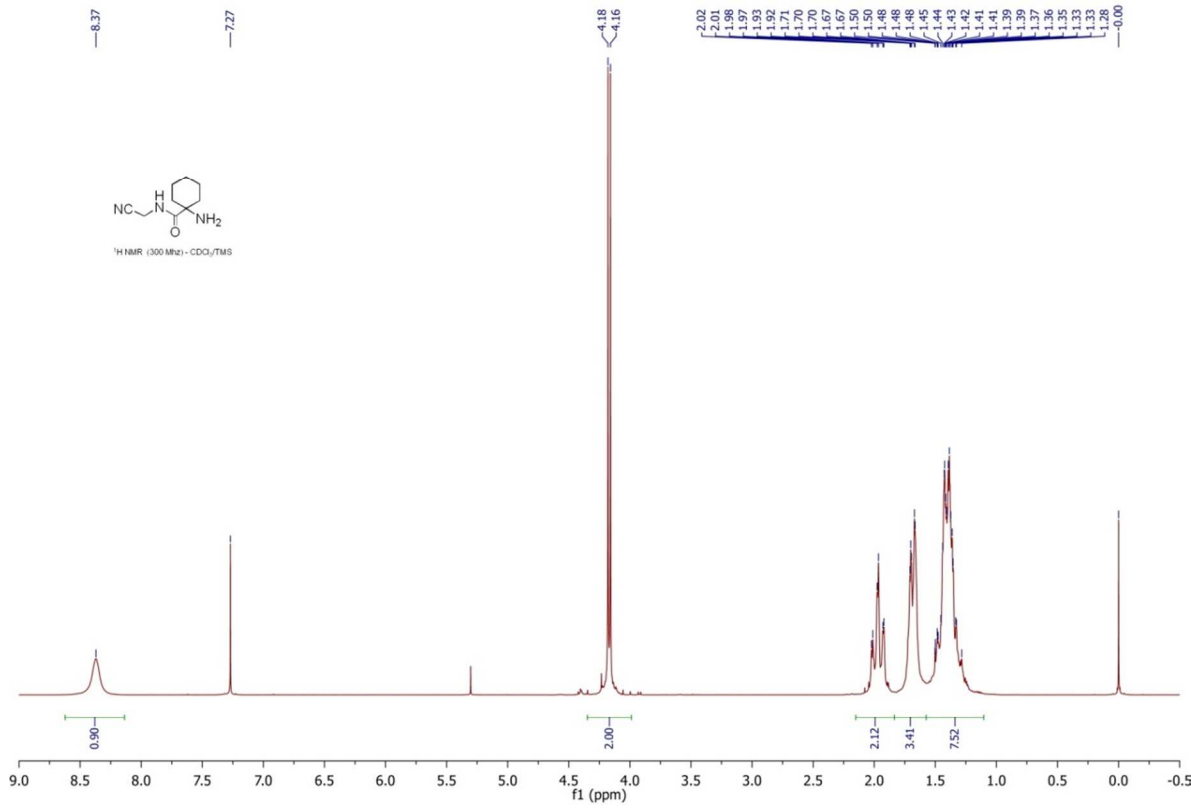
Compound 1



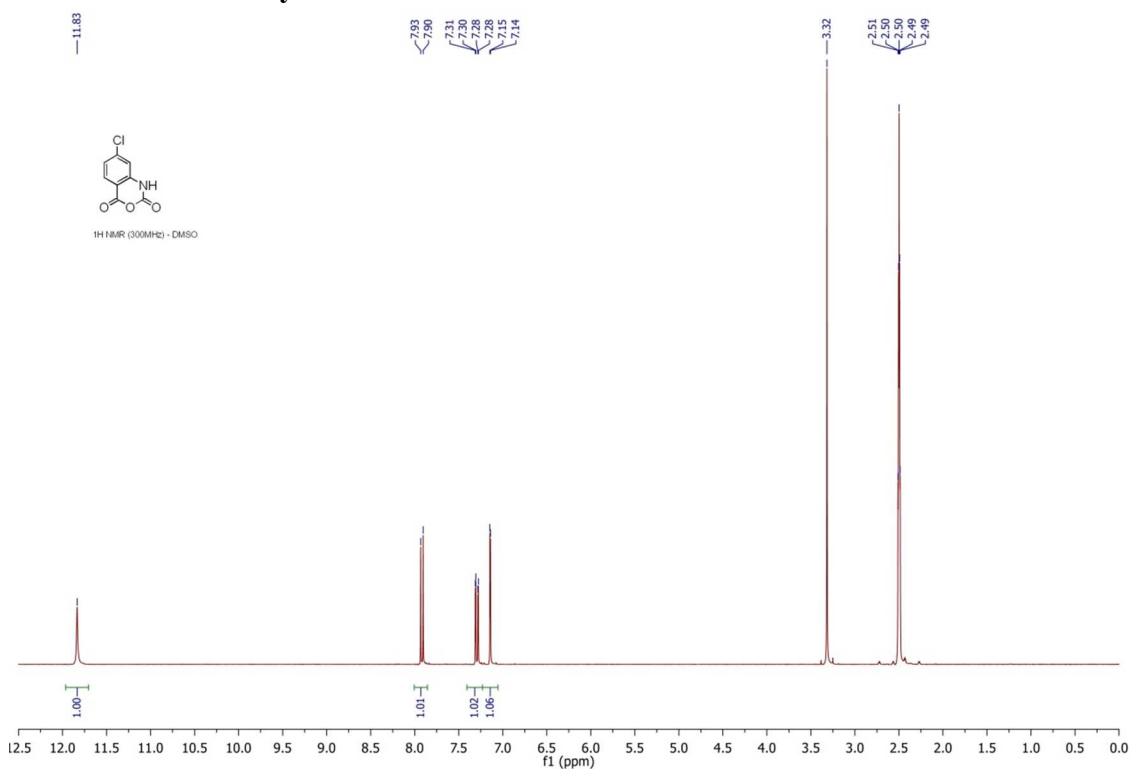
Compound 2



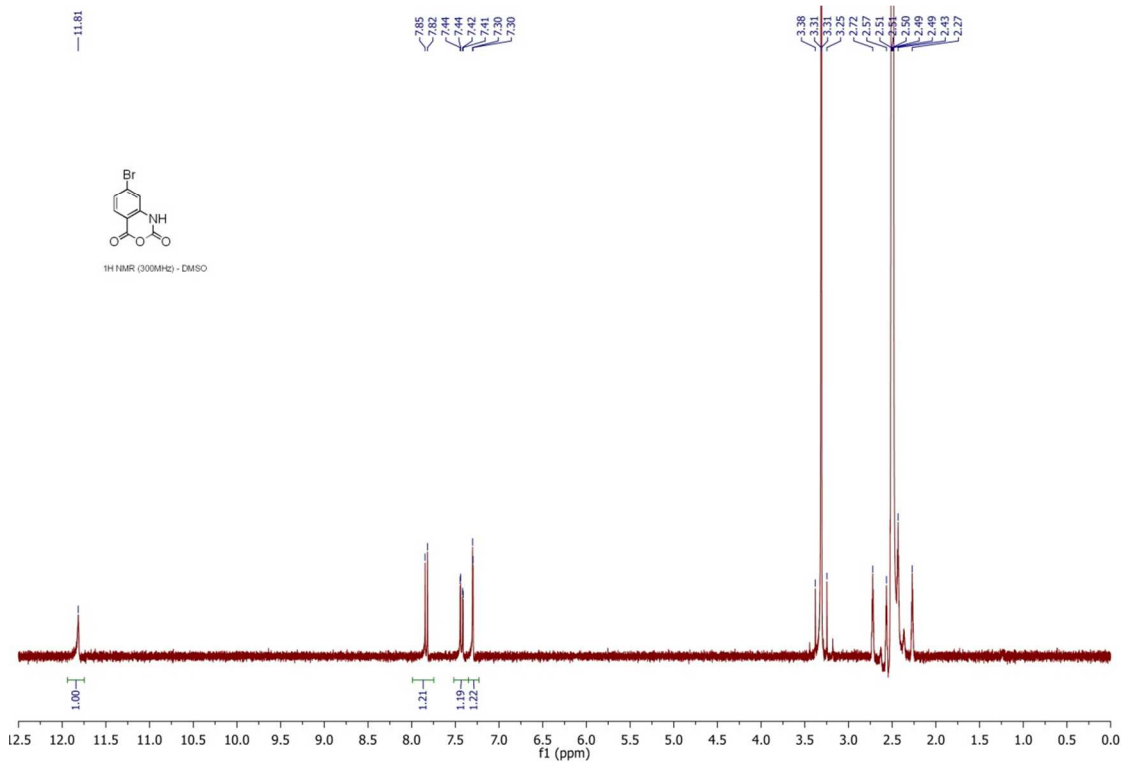
Compound 3



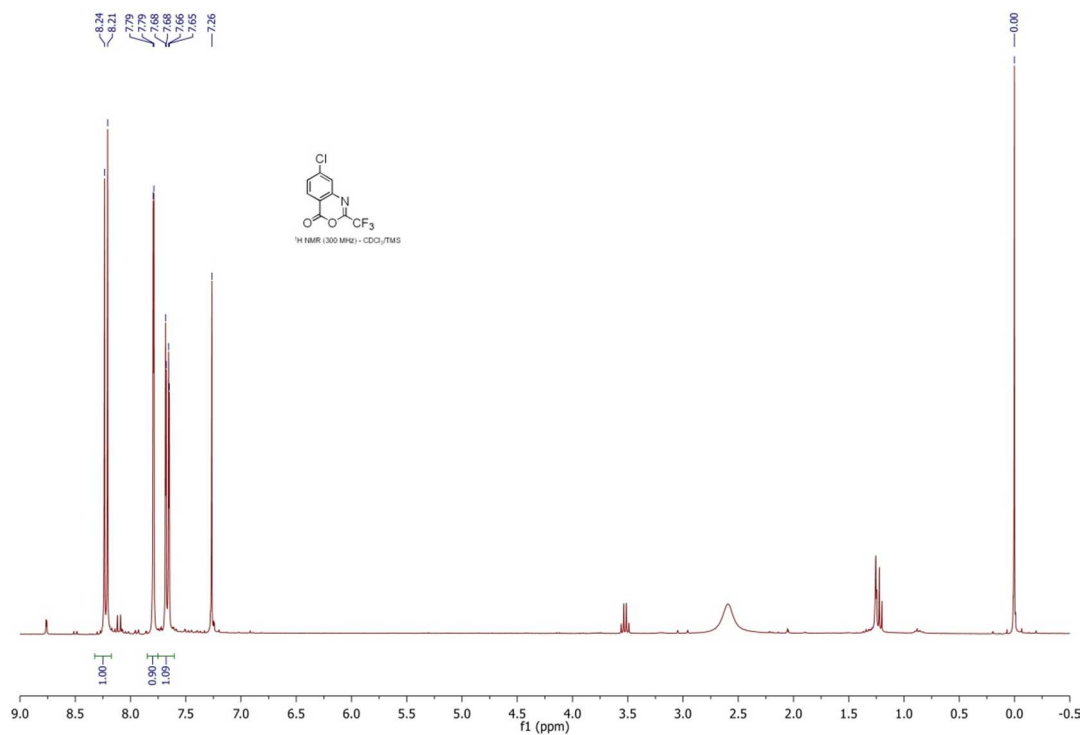
4-Chloroisatoic anhydride



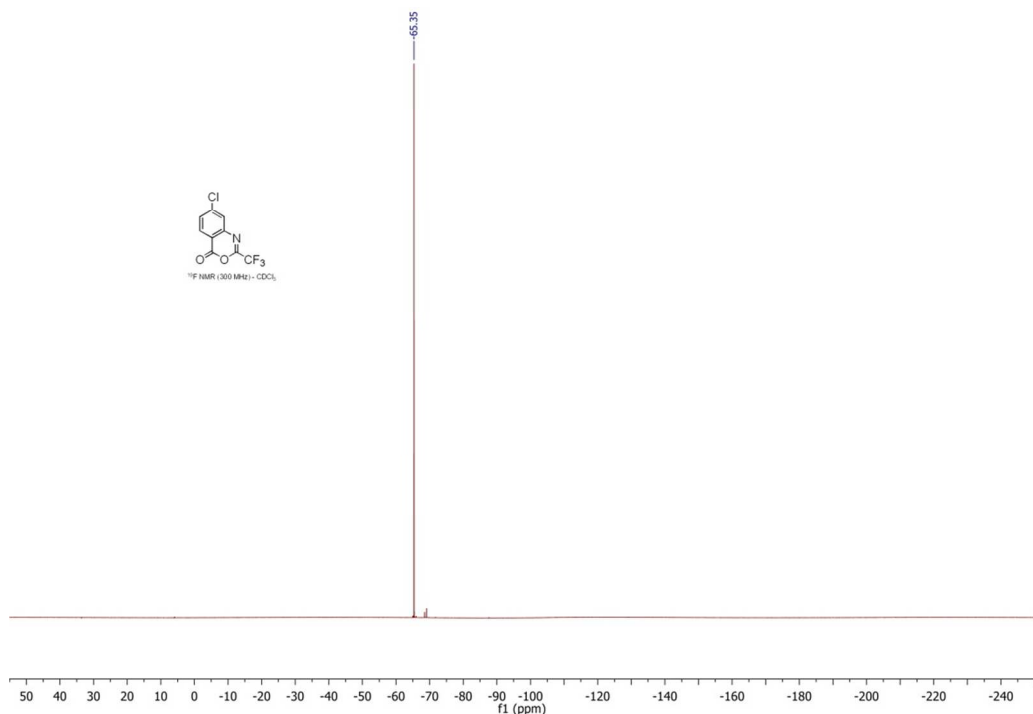
4-Bromoisatoic anhydride



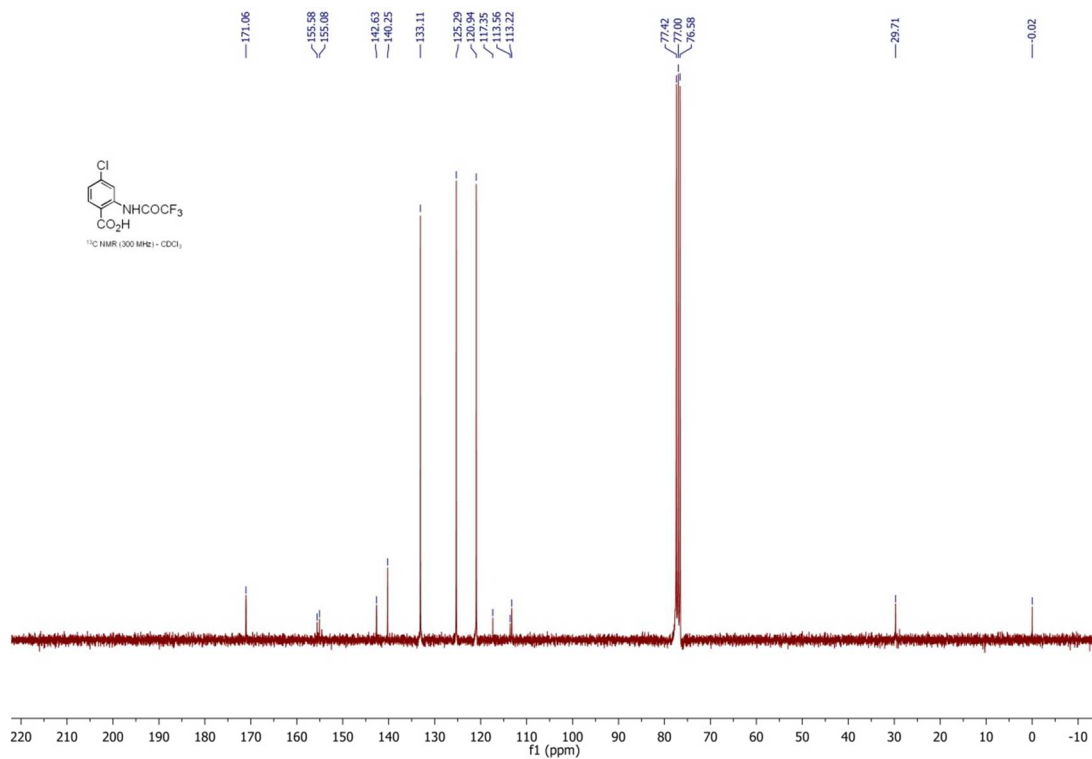
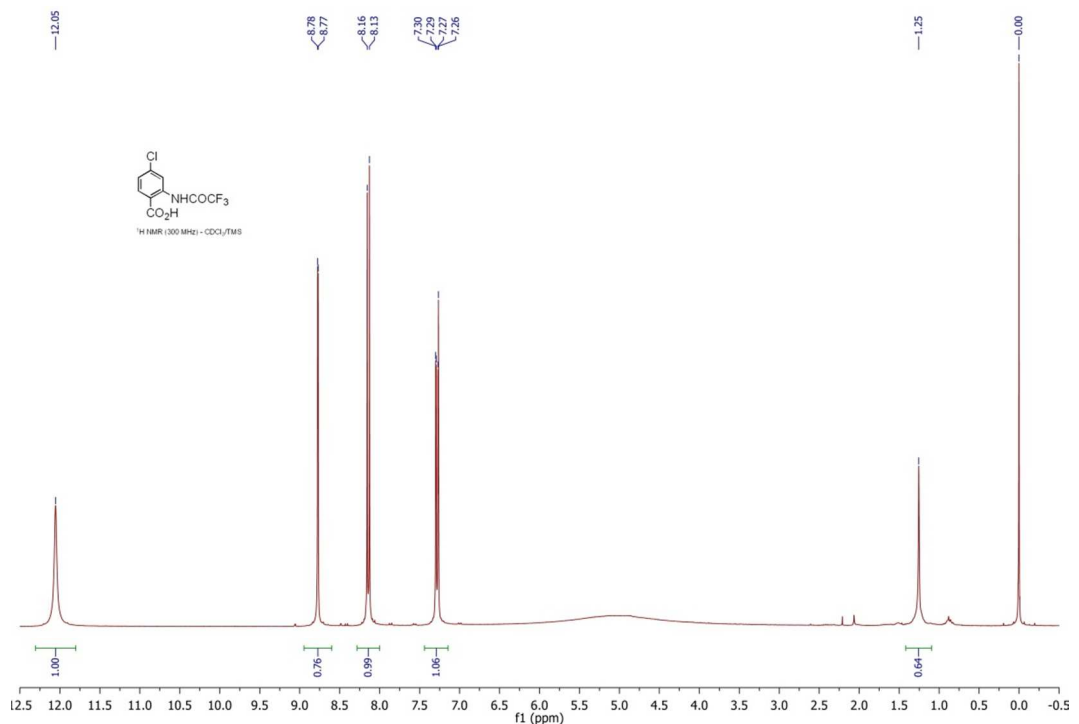
7-Chloro-2-trifluoromethyl-4*H*-3,1-benzoxazin-4-one

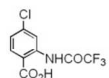


7-Chloro-2-trifluoromethyl-4*H*-3,1-benzoxazin-4-one

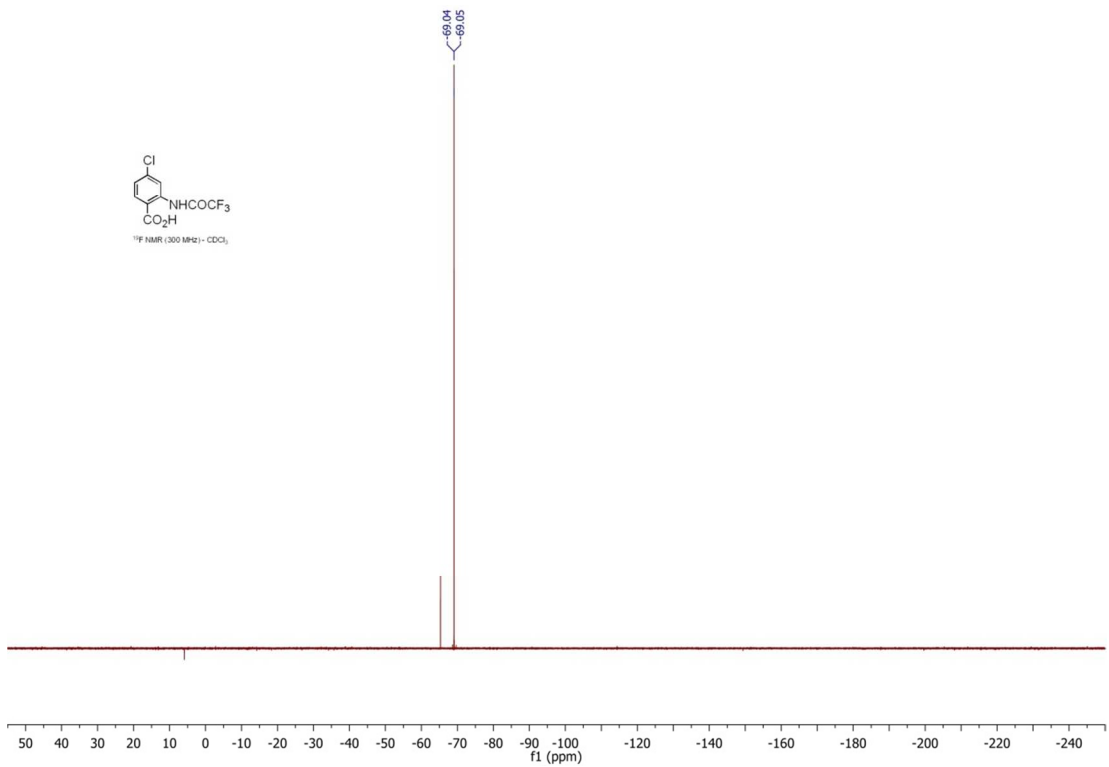


N-Trifluoroacetyl-4-chloroanthranilic acid

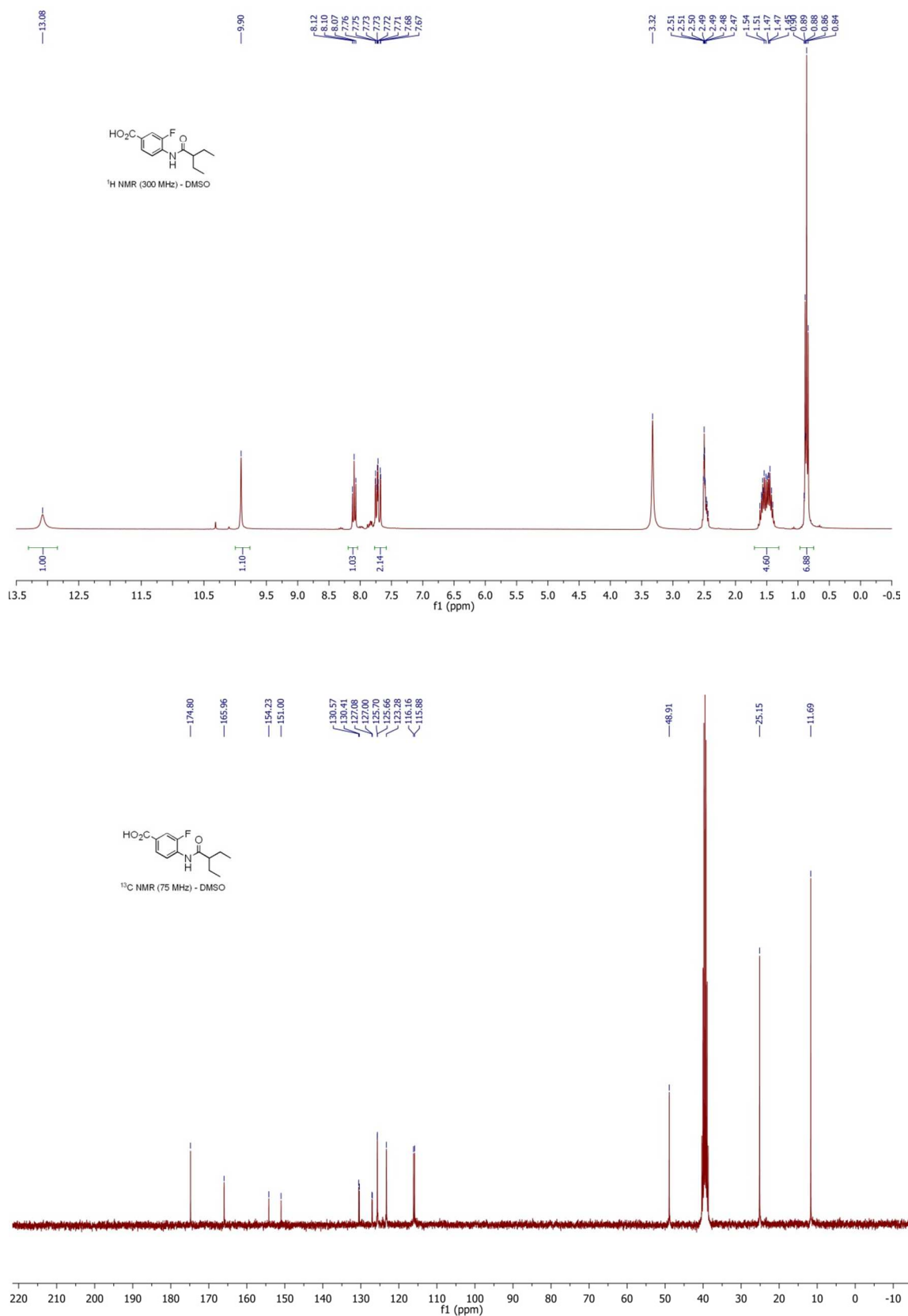


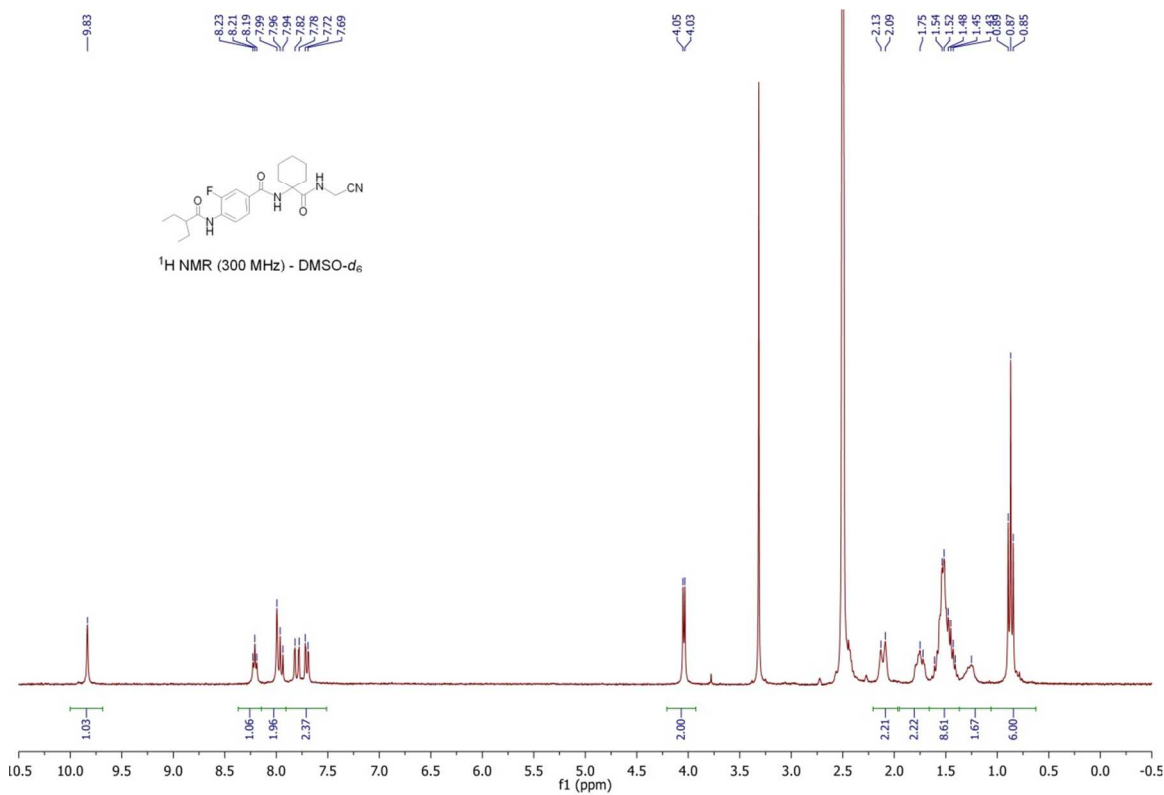
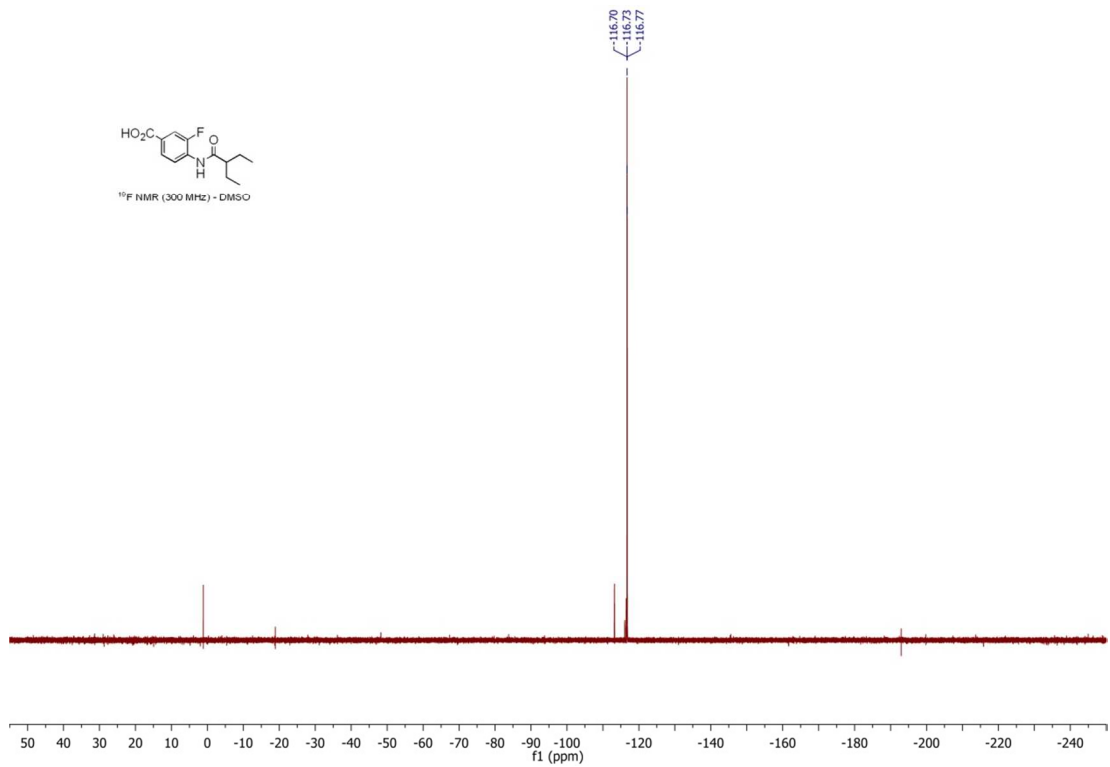


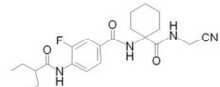
¹³C NMR (300 MHz), CDCl₃



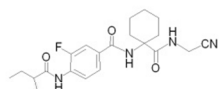
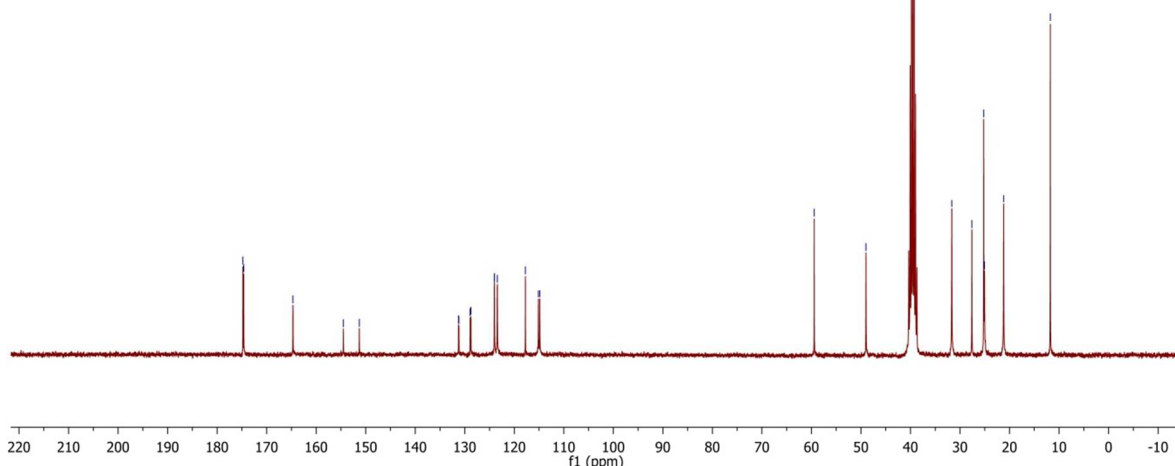
4-(2-Ethylbutyrylamino)-3-fluorobenzoic acid



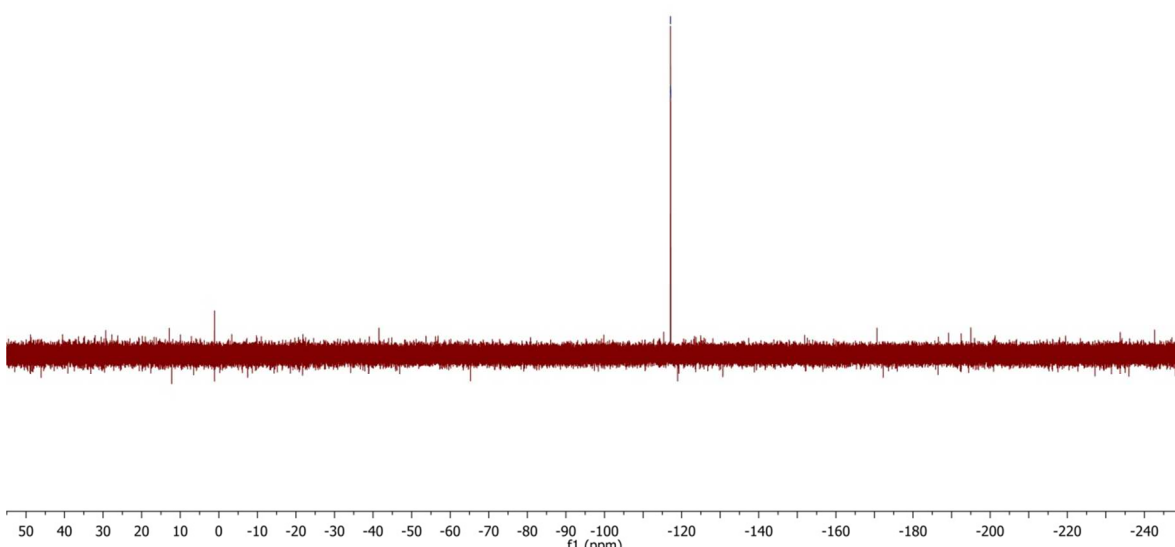




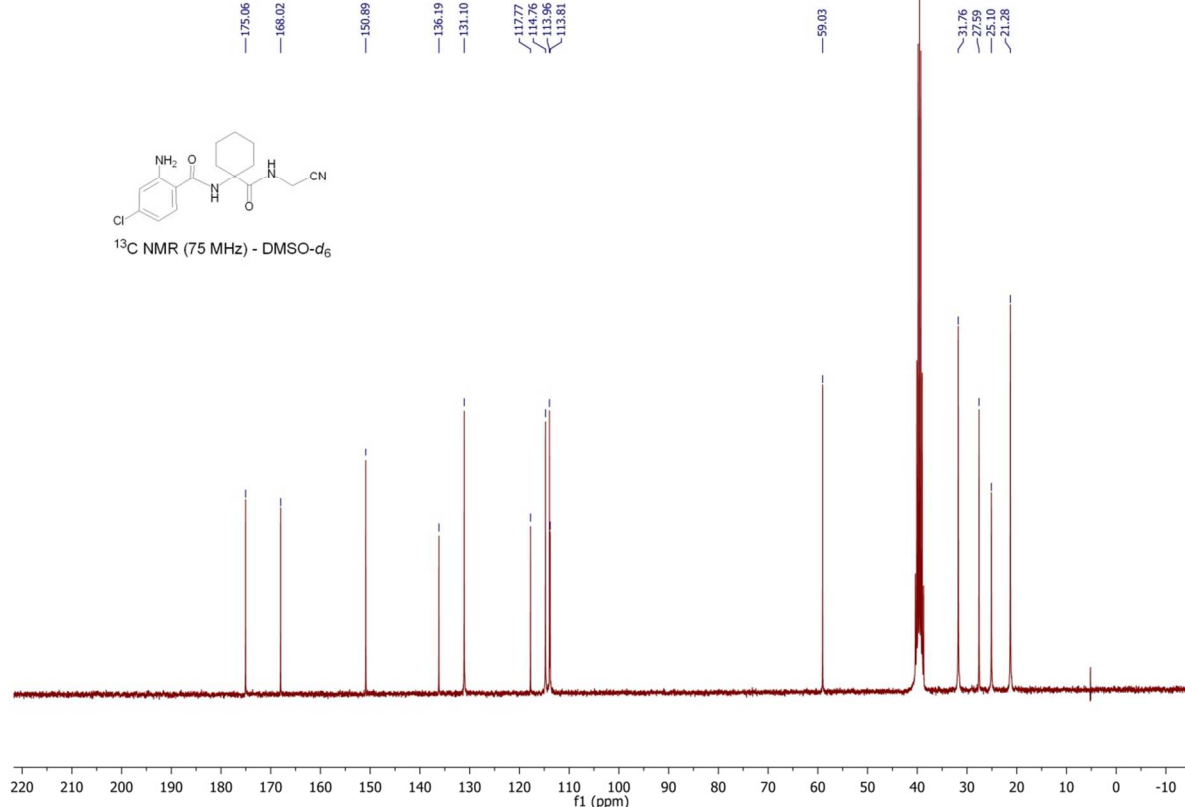
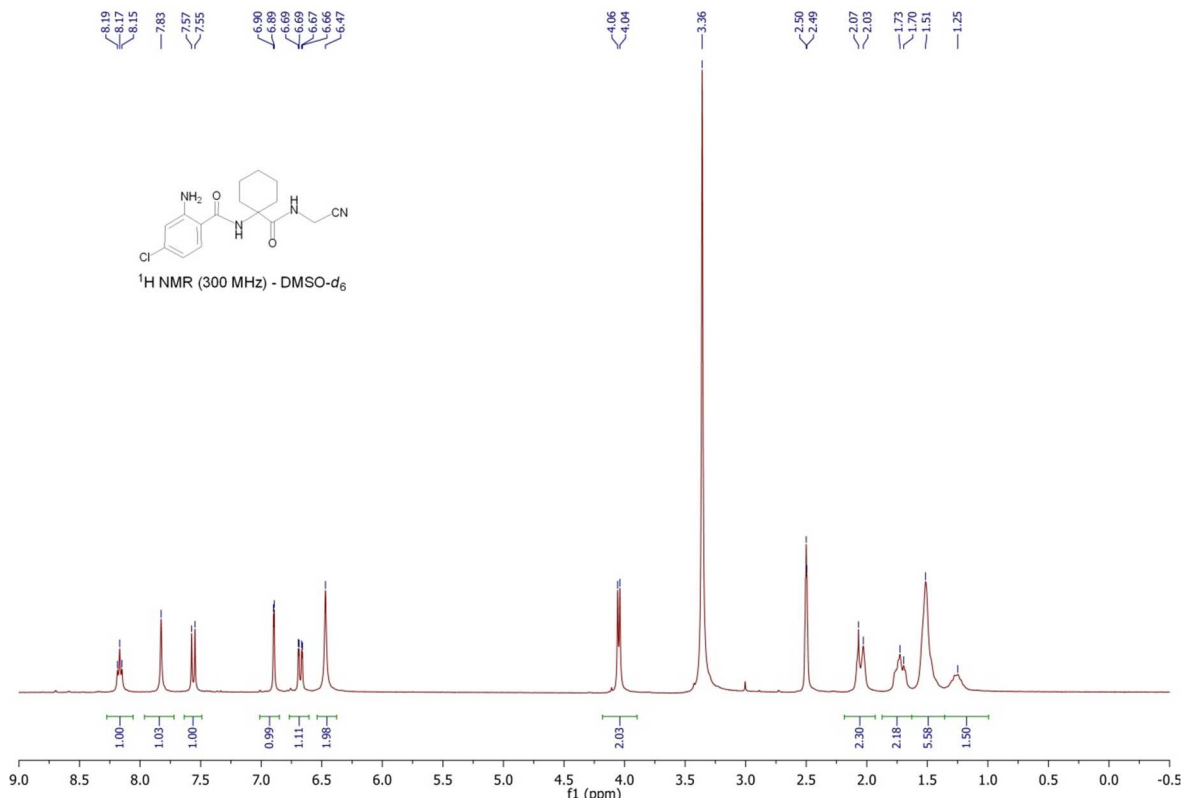
¹³C NMR (75 MHz) - DMSO-d₆



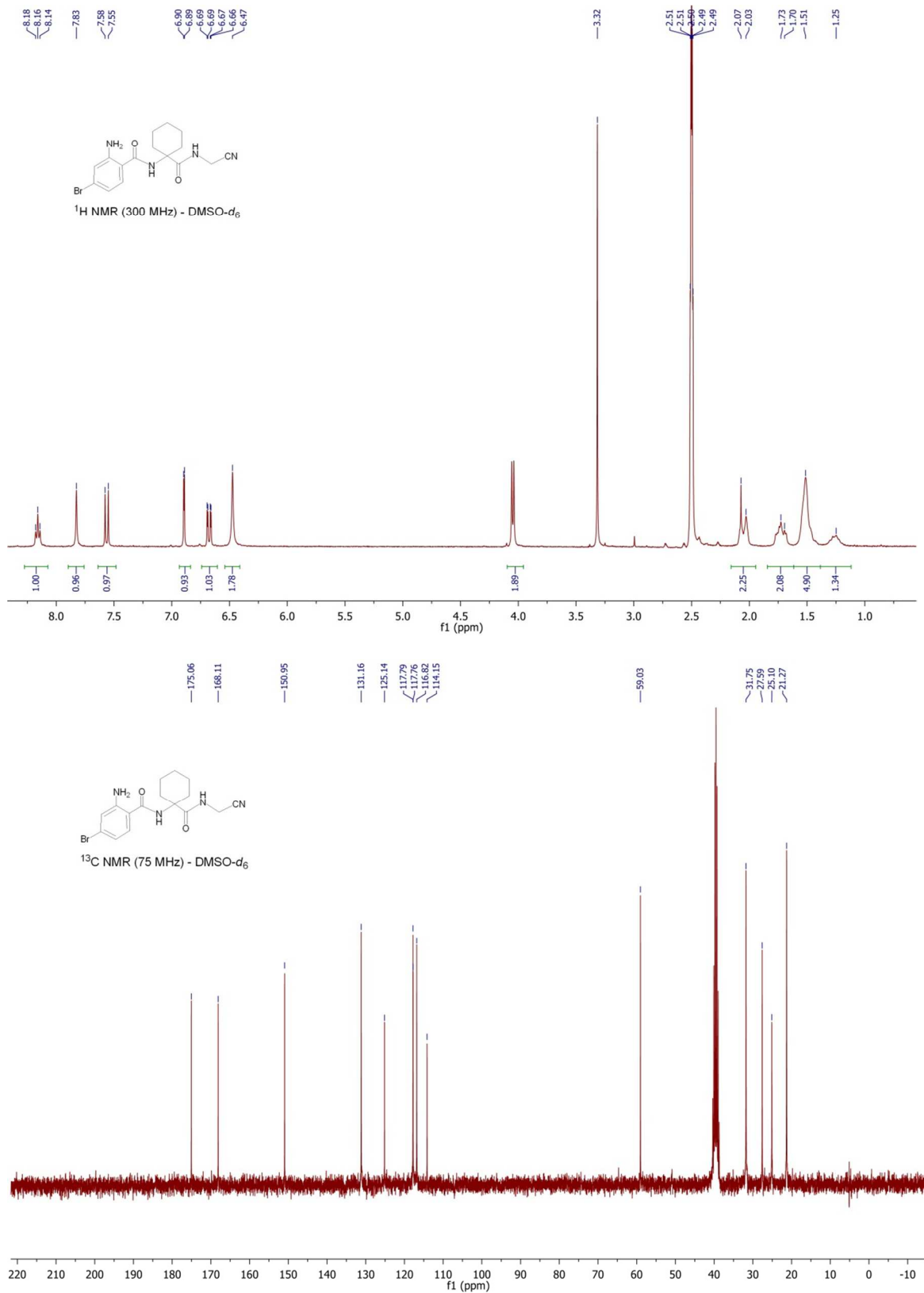
¹⁹F NMR (300 MHz) - DMSO-*d*₆



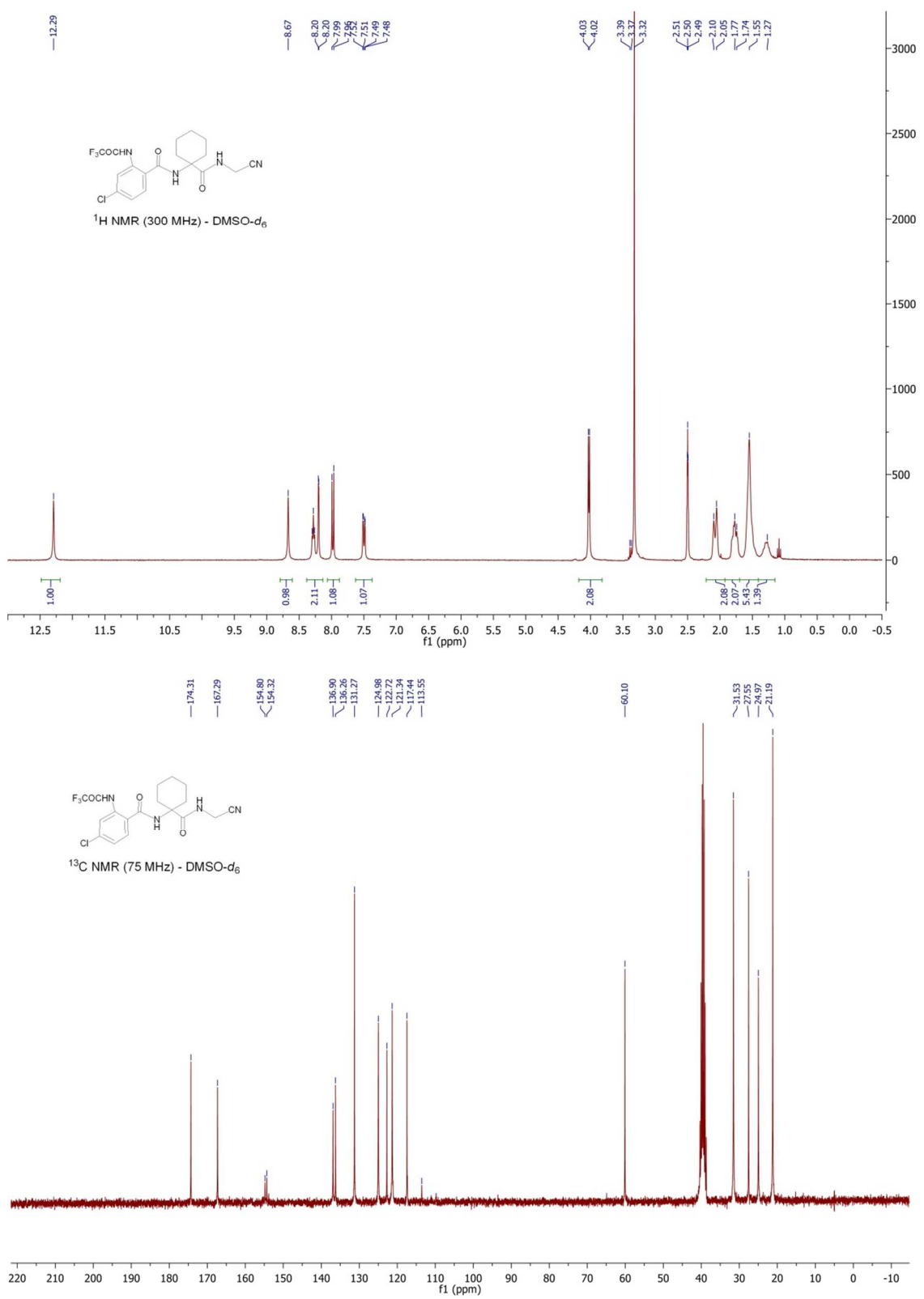
Compound 5

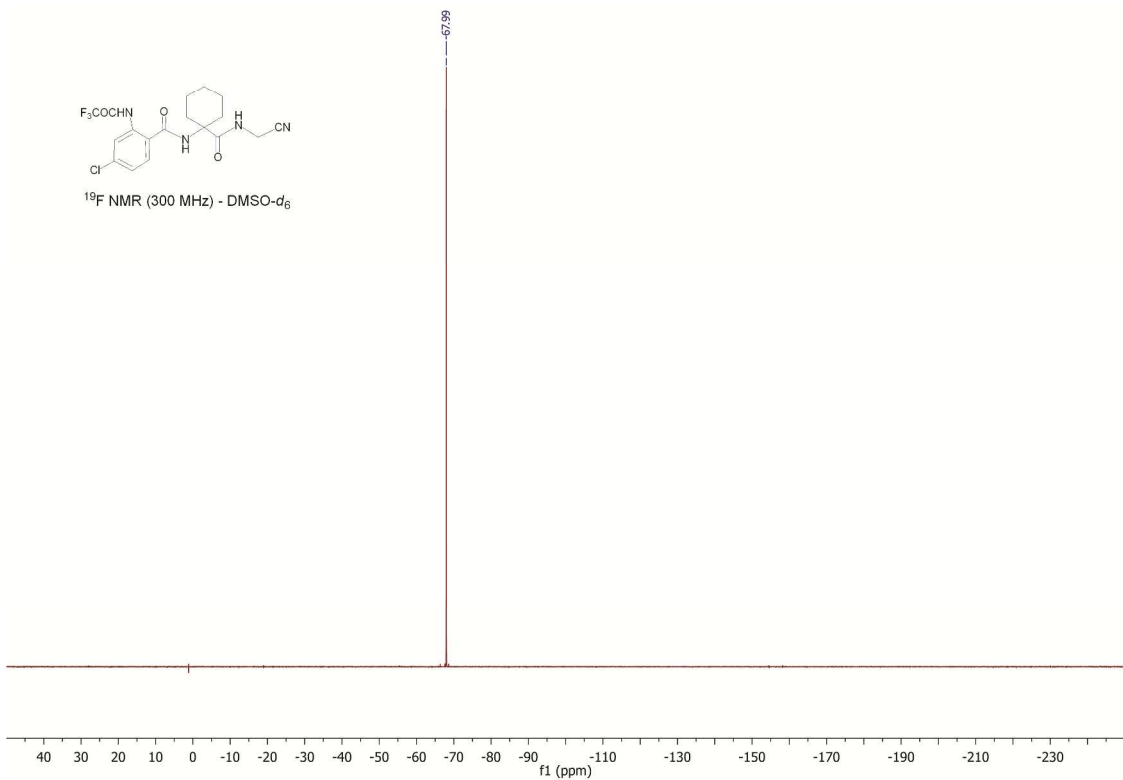


Compound 6

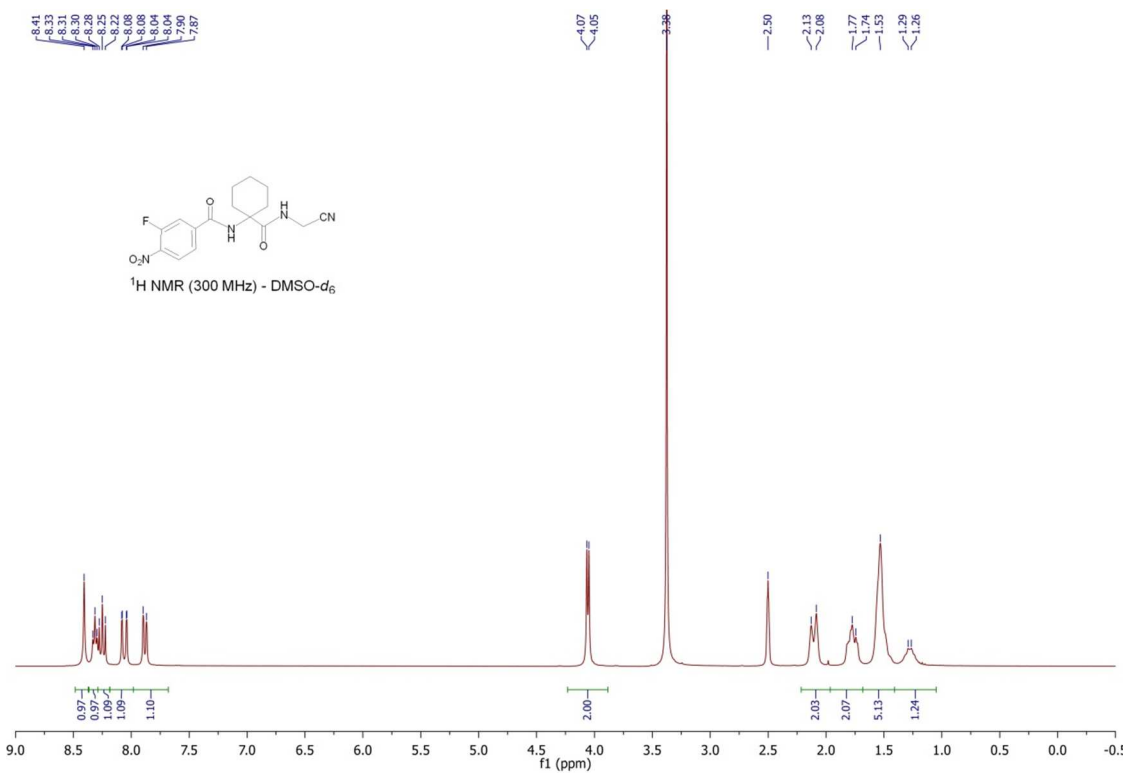


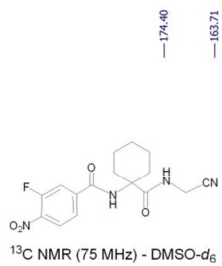
Compound 7



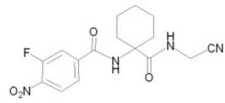
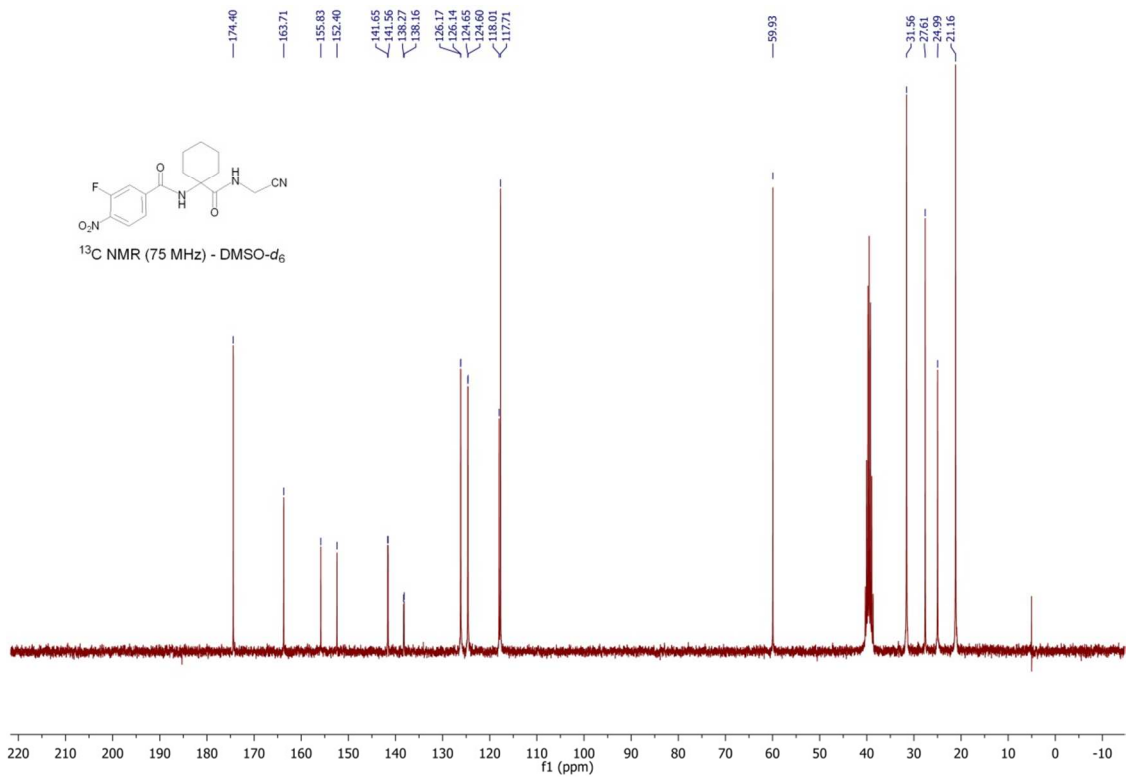


Compound 8

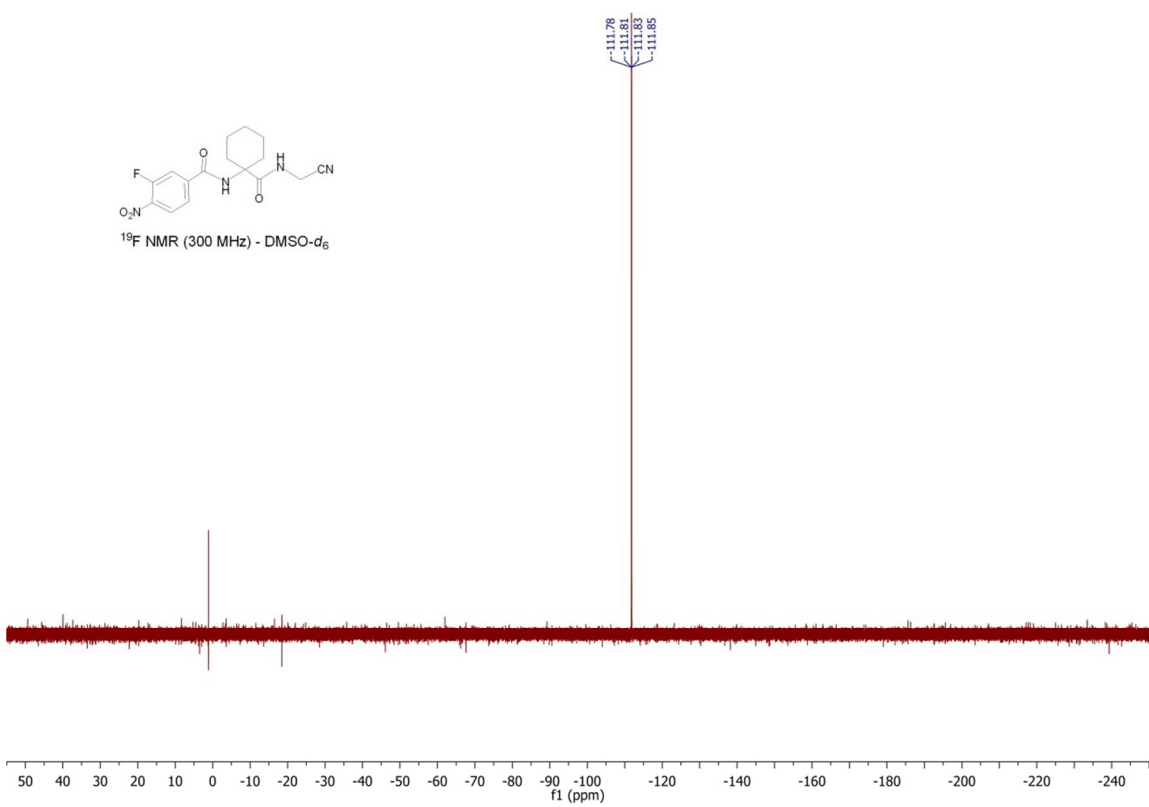




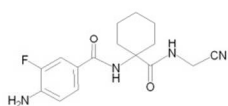
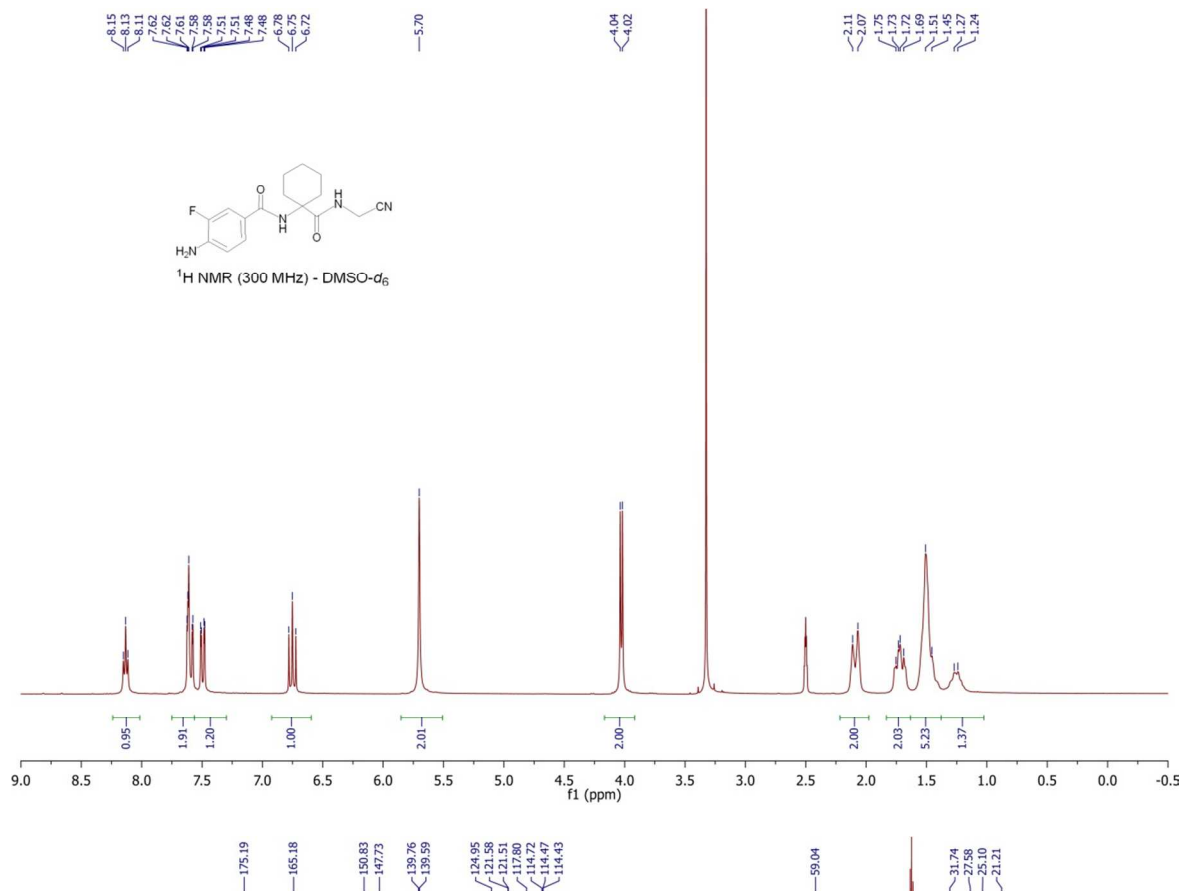
¹³C NMR (75 MHz) - DMSO-d₆



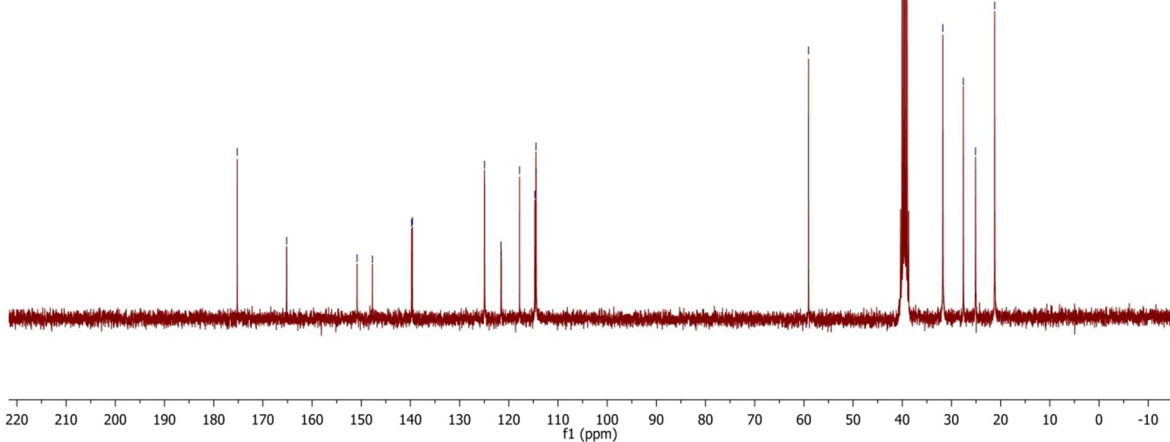
¹⁹F NMR (300 MHz) - DMSO-d₆

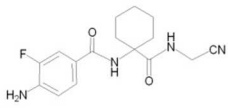


Compound 9

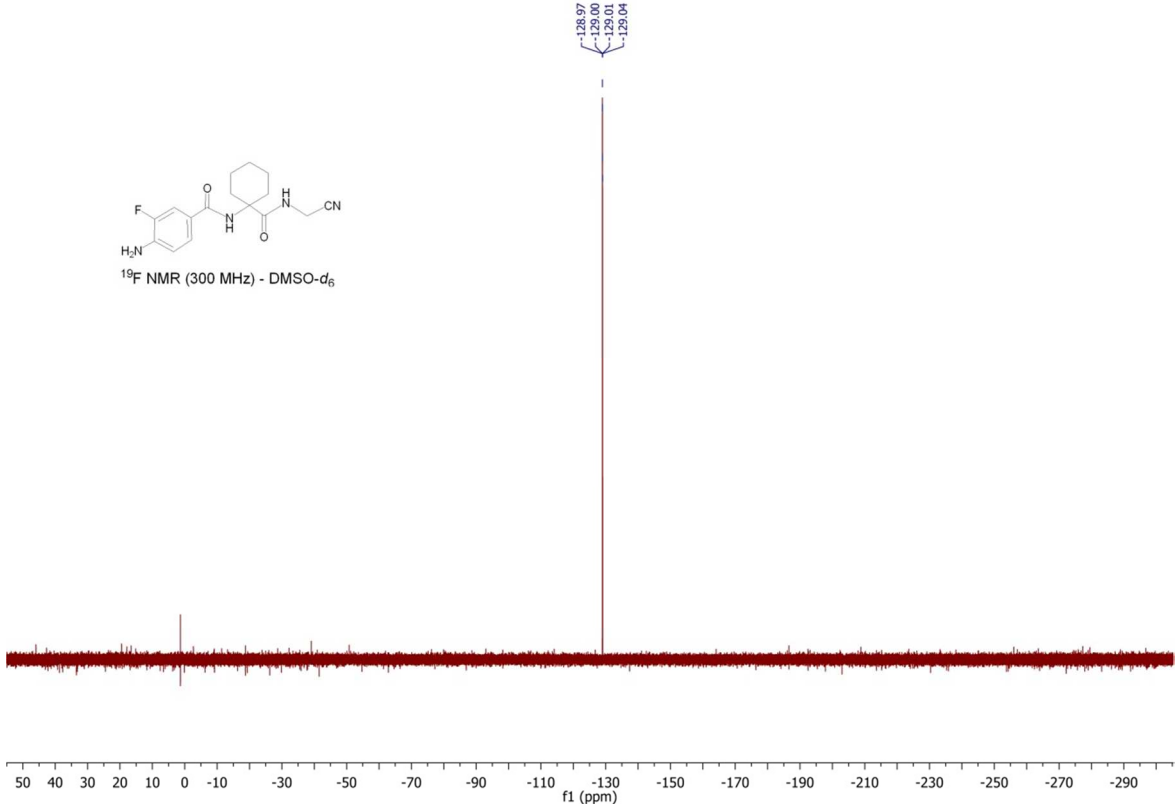


¹³C NMR (75 MHz) - DMSO-*d*₆

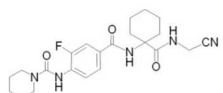




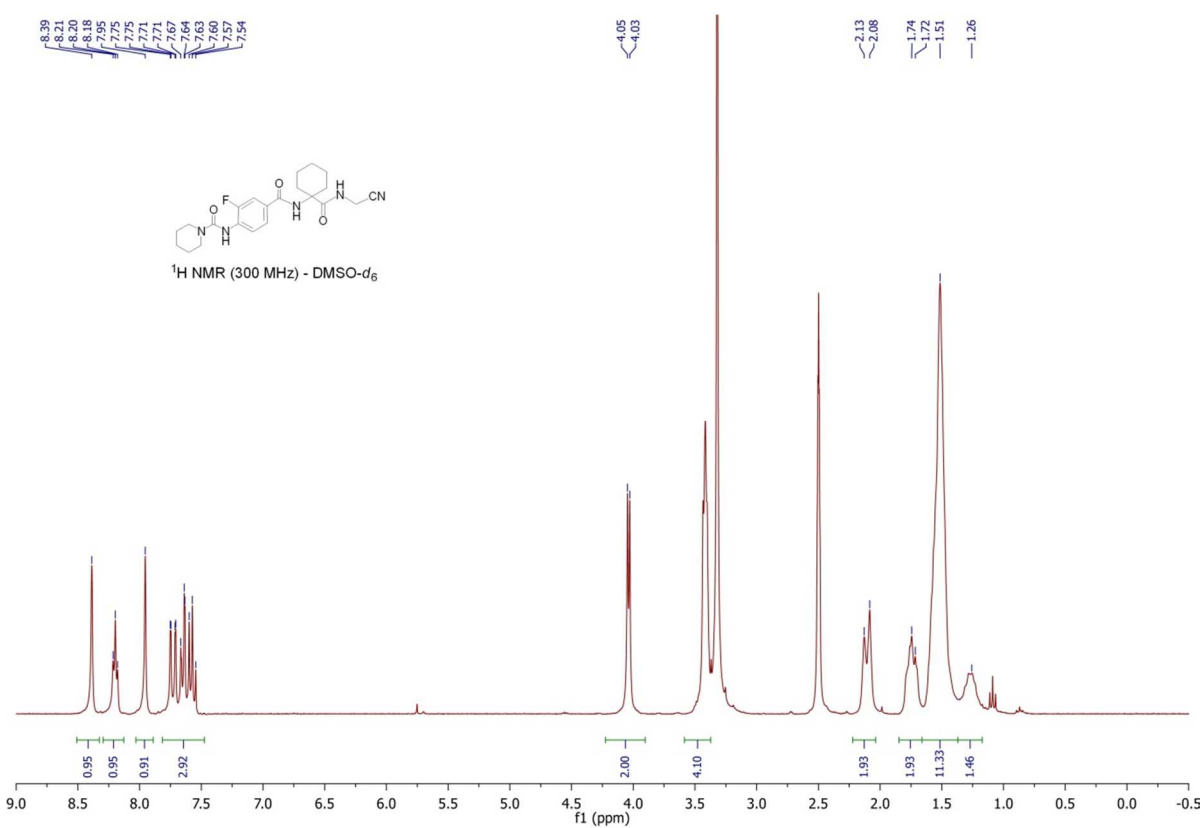
¹⁹F NMR (300 MHz) - DMSO-d₆

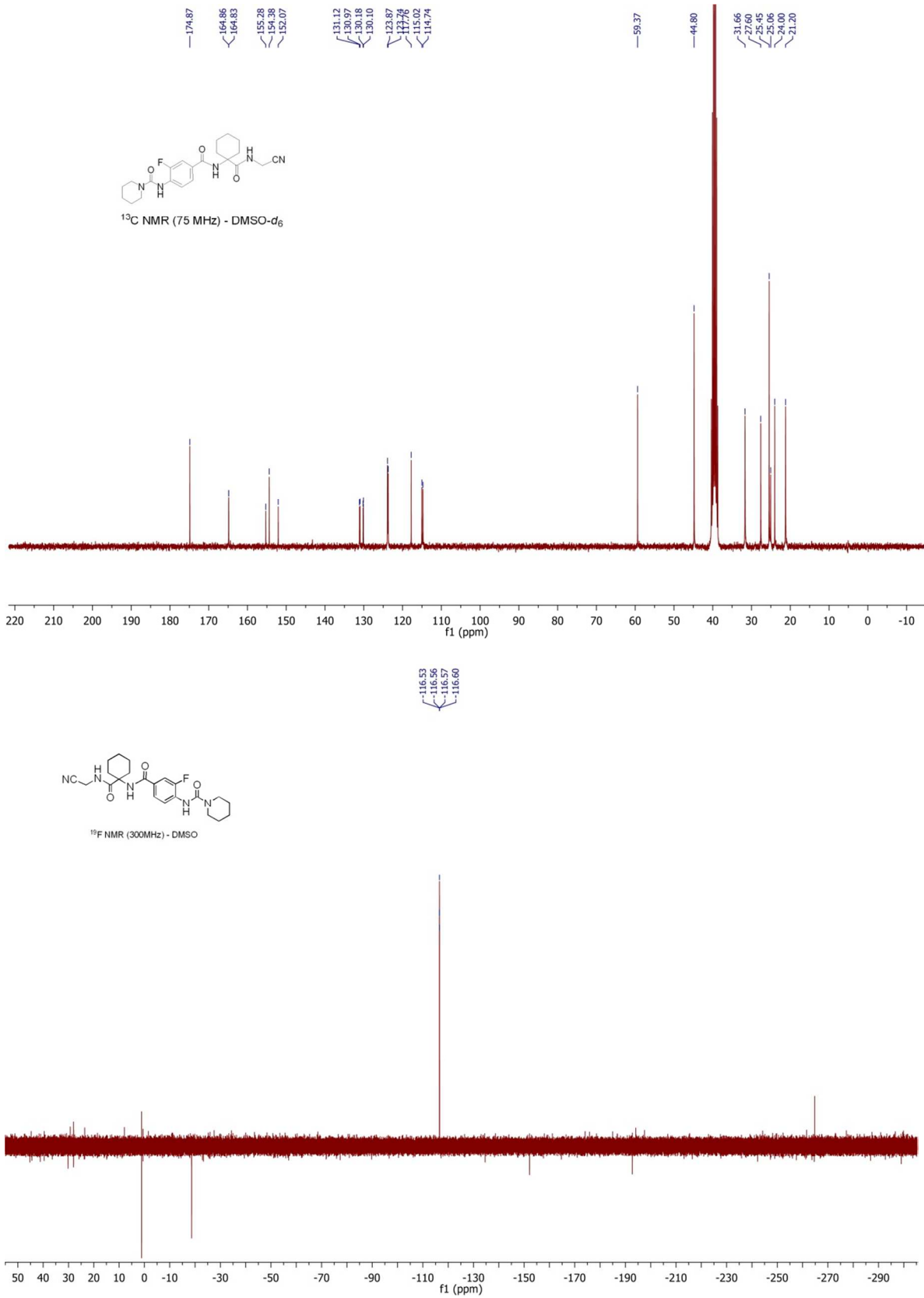


Compound 10

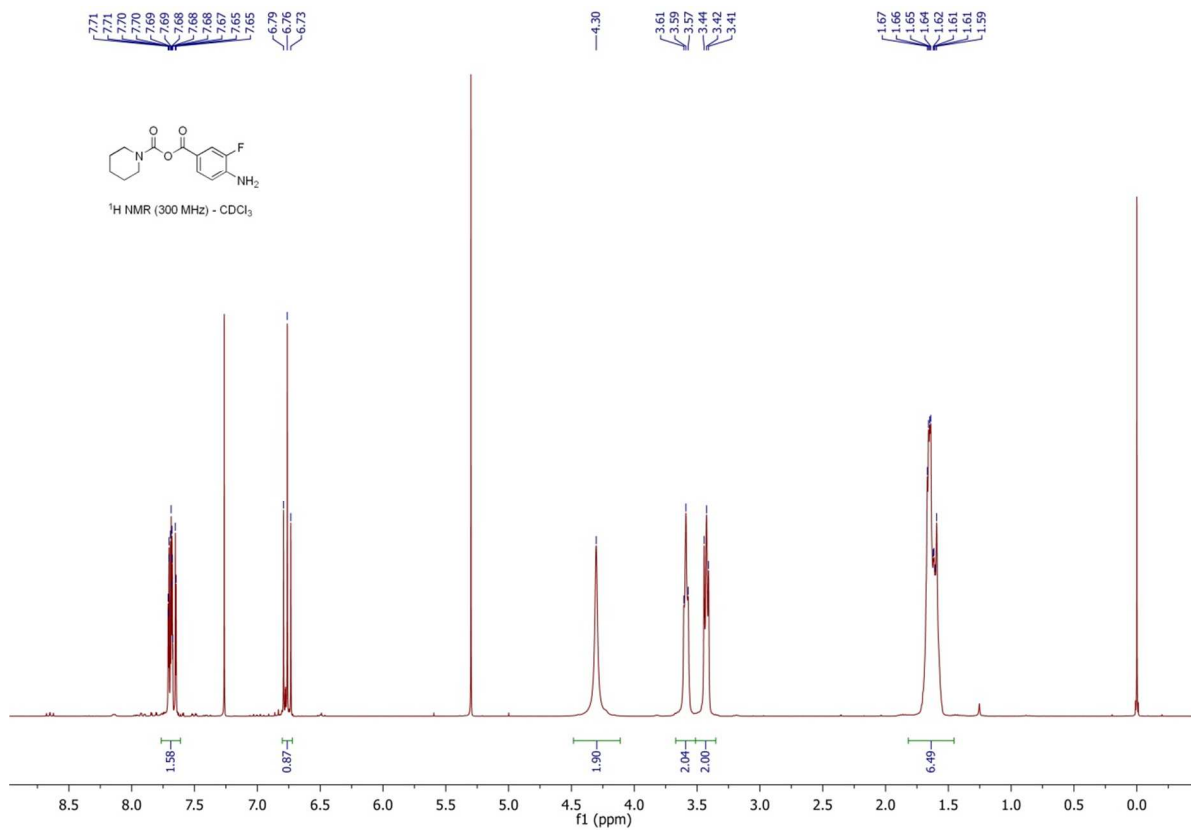


¹H NMR (300 MHz) - DMSO-d₆





Compound 12



Compound 13

